Machine-learning algorithms for the identification of visual field loss associated with the anti-seizure medication vigabatrin - a proof of concept.

John M Wild*[1], Philip EM Smith[2] and Carlo Knupp[1]

1. Cardiff Centre for Vision Sciences Research
   College of Biomedical and Life Sciences
   Cardiff University
   Cardiff
   CF5 6DE
   United Kingdom

2. The Alan Richens Unit
   Welsh Epilepsy Centre
   University Hospital of Wales
   Heath Park
   Cardiff
   CF14 4XW
   United Kingdom

* Corresponding author

John M Wild wildjm@cardiff.ac.uk
Philip E M Smith smithpe@cardiff.ac.uk
Carlo Knupp knuppc@cardiff.ac.uk

ABSTRACT

Background/ Aims The antiseizure medication, vigabatrin, is associated with visual field loss (VAVFL). However, the fields can be challenging to interpret due to unfamiliarity with the characteristics of the defect and/ or to difficulty in obtaining a reliable examination, particularly in patients with cognitive limitations associated with the epilepsy. Two machine-learning pattern recognition algorithms were developed to identify VAVFL, objectively.

Methods The algorithms adhered to the European Medicines Agency-approved protocol for the detection of VAVFL (Three Zone Age Corrected Full Field 135 Screening Test [FF135] and the Central C30-2 Threshold Test [C30-2T] with the Humphrey Field Analyzer). Each algorithm compared the similarity of the measured field from each eye to that of modelled reference patterns of VAVFL, matched for equivalent severity, and objectively derived from a previously described case series of 123 adults. The algorithms were augmented by the optional inclusion of symmetrisation, a signal-to-noise enhancement technique based upon the between-eye mirror image symmetry of VAVFL. Utility of the algorithms for identifying VAVFL was evaluated against a case series of 89 consecutively identified individuals stratified across six diagnostic categories including homonymous and glaucomatous losses.

Results The algorithms exhibited excellent agreement with a 'gold standard' clinical interpretation (sensitivity and specificity: FF135, 22/23; 30/30; C30-2T, 17/18; 48/51). Symmetrisation was particularly useful in identifying VAVFL when perimetric learning or fatigue influenced the outcome for one eye and for visualisation in the presence of concomitant homonymous loss.

Conclusion The directly-interpretable machine learning outcome correctly identified VAVFL and could assist patient management in community (neuro-)ophthalmology.

WHAT IS ALREADY KNOWN

Deep learning Artificial Intelligence techniques have long been applied to ophthalmology. However, such techniques are ‘black boxes’ in that the manner by which the neural network architecture achieves the outcome is challenging to interpret which, in turn, is a limiting factor for their adoption in clinical practice. The visual field loss associated with the antiseizure medication, vigabatrin, can be difficult to interpret due to unfamiliarity with the characteristic pattern of loss and/ or to difficulties in obtaining a reliable outcome to the perimetry due to the cognitive limitations accompanying the epilepsy.

WHAT THIS STUDY ADDS

Machine-learning algorithms are described which enable a directly interpretable clinically based objective classification of both the presence and the severity of vigabatrin-associated visual field loss (VAVFL) obtained with the European Medicines Agency-approved perimetric protocol. This objective classification exhibited close agreement with a ‘gold standard’ subjective clinical opinion across a validation case series of 89 individuals. A signal-to-noise enhancement technique, symmetrisation, improved the outcome from poorly recorded visual fields and also from those with concomitant homonymous loss.

HOW THIS STUDY MIGHT AFFECT RESEARCH, PRACTICE OR POLICY

These machine learning algorithms have the potential to increase the sensitivity and specificity for the designation of VAVFL, thereby improving the assessment of the benefit:risk profile of vigabatrin, i.e. seizure control verses ocular toxicity. The algorithms could also assist community clinicians to become familiar with the characteristics of the field loss.

INTRODUCTION

The antiseizure medication vigabatrin is used as adjunctive therapy for refractory focal impaired awareness seizures (FIAS)[1] and for infantile epileptic spasms syndrome, particularly those arising from tuberous sclerosis complex. [2]

The use of vigabatrin is predicated upon the basis that the improvement in seizure control outweighs the risk of the associated ocular toxicity. [3] The toxicity manifests as a characteristic pattern of visual field loss, [4, 5] corresponding thinning of the peripapillary retinal nerve fibre layer [6-10] and abnormalities of the electroretinogram, the most sensitive and specific of which is the light-adapted 30Hz flicker. [11, 12] Other signs can include an inverse optic atrophy, [13, 14] retinal pigment epithelial changes, [4, 5] retinal arterial narrowing [4,15,16] and retinal surface wrinkling, [15, 16] but these signs are often not discernible until advanced visual field loss is present. The mechanism of the toxicity is unknown.

The risk of vigabatrin associated visual field loss (VAVFL) in adults, modelled from cross-sectional evidence, increases rapidly from approximately the first 2 years (2kg cumulative dose) of therapy [17-19] and reaches 70%-80% after approximately 5-6 years (5-6kg cumulative dose). [18, 19] The severity of VAVFL is seemingly independent of the extent of exposure to vigabatrin [20].

VAVFL comprises a bilateral, clinically symmetrical, concentric constriction which exhibits a continuum of severity, encroaching centripetally, initially temporally and then along all meridians, from the peripheral to the central field. [4, 5, 20] The loss within the central field, by standard automated perimetry, manifests as a binasal annular defect of varying severity, which initially occurs inferior-nasally, and, with subsequent temporal encroachment, can result in a concentric defect to within approximately 15° from fixation. [4, 5, 20] The prevalence of VAVFL may be lower in children; [3] however, it is generally accepted that the characteristics of the field loss are the same as those in adults. [20] VAVFL is slowly progressive, [20-22] irreversible but non-progressive on withdrawal from the medication [23, 24] and asymptomatic until the loss is severe. [4]

Interpretation of VAVFL can be particularly challenging since the cognitive constraints/ limitations associated with the epilepsy can adversely impact upon the outcome of the visual field examination.

The measurement, itself, is further confounded by the normal physiological variability which increases with increases in eccentricity of the stimulus from fixation, in the depth, and in the overall severity, of the field loss. [25] Additional variability arises from such factors as the perimetric learning [26] and fatigue [27] effects, incorrect optical correction, [28] anxiety [29] and incorrect prior instruction to the patient. [30] A poor-quality outcome can mimic, mask or exaggerate the presence of 'true' VAVFL thereby hindering the evaluation as to the presence and/ or severity of VAVFL and/ or of any progressive loss. The presence of concomitant field loss, most commonly homonymous loss, is a further confounding factor.

A false-positive interpretation for VAVFL will most likely lead to the discontinuation of vigabatrin with the associated potential for poor seizure control. A false-negative interpretation, arising from the use of an inappropriate type of perimetry [31, 32] and/ or from the erroneous assumption that the recorded field loss arises from afferent system comorbidity associated with severe refractory epilepsy [33] will lead to continued usage of the drug with the potential for an exacerbation of the toxicity.

Clearly, there is a need for an objective method for evaluating the outcome of perimetry in patients exposed to vigabatrin. The aim of the study, therefore, was threefold. First, to develop machine-learning algorithms with well-defined output criteria, based upon pattern recognition, for the objective evaluation of VAVFL, derived with the European Medicines Agency (EMA)-approved perimetric protocol for use with vigabatrin. [34] By these means, VAVFL would be differentiated from other types of visual field loss and from apparent loss arising from variable/ poorly performed perimetry. Second, to validate the algorithms for the identification of VAVFL across a case series of individuals with FIAS, either never or previously exposed to vigabatrin, and with or without concomitant homonymous field loss; and, also, as a control, those with a negative history for epilepsy but with either homonymous or glaucomatous field loss. Third, to augment the algorithms, by the removal of extraneous factors adversely influencing the measured field, using a signal-to-noise enhancement technique, symmetrisation, based on the between-eye location-specific mirror image symmetry of VAVFL [20].

MATERIALS AND METHODS

Concept of the pattern recognition algorithms

The concept of the pattern recognition algorithms is to indicate, objectively, whether the appearance of any given measured pair of fields from an individual exposed to vigabatrin, matched the modelled reference pattern of VAVFL of equivalent severity.

Compilation of the modelled reference pattern of VAVFL

The modelled reference pattern of VAVFL was derived from a locked case series of 123 individuals attending the Alan Richens Unit of the Welsh Epilepsy Centre, University Hospital of Wales, Cardiff, UK, and associated clinics. [20] All conformed to robust inclusion criteria [20] including visual field examination with an EMA-approved perimetric protocol for the detection of VAVFL,[34] namely the Three Zone Age Corrected Full Field 135 Screening Test (FF135) and/ or the Central C30-2 Threshold Test (C30-2T) with the Humphrey Field Analyzer (Section S1 in the Supplementary Material). The fields had been reviewed according to the aforementioned description of VAVFL and masked to the antiseizure medication history, by a panel of three individuals, independently of one another, comprising a consultant ophthalmologist, either of two consultant neurologists, and a clinical visual scientist, who were all highly experienced in the interpretation of VAVFL. The VAVFL was required to exhibit a consistent appearance between suprathreshold and standard automated perimetry. In all cases, but particularly for those in which the loss was concentric within the central field, the evaluation was confirmed by exclusion of confounding factors such as poor compliance and of other ophthalmologic or neurologic causes determined at clinical examination by the corresponding lead clinician including, as appropriate, ocular electrophysiology and whole brain MRI. The modelling process, including the mathematical manipulations [20] is summarised in the Supplementary Material. The summary statistics for the demographics of the 123 individuals are shown in Table 1 (shaded row).

Compilation of the pattern recognition algorithms

Separate algorithms were developed for the FF135 and for the C30-2T.

The measured fields from each of the 123 individuals, considered as a right and left eye pair, were ranked for each type of perimetry from the least to the most severely affected in terms of the total

number of locations exhibiting abnormality. The locations for the FF135 were transformed in terms of a weighting whereby a normal response was designated as 0.0, relative loss as 0.75 and absolute loss as 1.00. The corresponding weighting for the C30-2T was based upon the probability level of the Pattern Deviation Probability Map. A normal response was weighted as 50; $p \leq 5\%$ as 95; $p \leq 2\%$ as 98; $p \leq 1\%$ as 99 and $p \leq 0.5\%$ as 99.5. The transformed values for each type of perimetry represented the optimum approach from a number of different exploratory iterations.

The median outcome at each location, in the right and left eyes separately, for each type of perimetry was then calculated for each 10 successive pairs of ranked fields (i.e., 1-10, 2-11, 3-12 etc). This process resulted in 78 pairs for the 87 individuals who had undergone the FF135 and 90 pairs for the 99 individuals who had undergone the C30-2T.

The ordinate of the plots from each algorithm represented the Euclidian distance of the measured pair of fields of an individual, across all stimulus locations, from the modelled reference pair of fields, matched for severity of loss. The abscissa represented the severity of the field loss.

The algorithms additionally compared the Euclidian distance of the measured pair of fields to a set of randomly generated pair of reference fields for each level of severity. The randomly generated fields were achieved for each type of perimetry by separately disaggregating the spatial configuration of the stimulus locations for each of the modelled reference pair of fields, and then randomising each array 10000 times to generate 10000 fields. The distance of each of the randomly generated pairs of fields from the modelled reference pair of fields, matched for severity, was then expressed in terms of the mean ±3SDs at each severity and inserted into the algorithm. The region inside ±3SDs thus contained pairs of fields that did not exhibit the modelled reference pattern of VAVFL at any level of severity and those outside -3.0SDs represented measured pairs of fields exhibiting VAVFL beyond chance at $p<0.0015$.

Symmetrisation of the measured field

Symmetrisation is a signal-to-noise enhancement technique which has previously been applied to VAVFL in order to reduce the adverse impact of extraneous factors on the measured field. [20] The

outcome at each between-eye mirror symmetric location of the measured field is averaged according to a previously derived protocol (Section S2 and online supplemental figure S1 in the online supplemental material). The assigned values across all locations are then re-compiled to form the symmetrised pair of fields for the given individual for the given type of perimetry. The resultant symmetrised pair of fields are then compared to the modelled reference pair of fields.

Validation case series

The sensitivity and specificity of the algorithms for the identification of VAVFL from the normal field and from different types of visual field loss were evaluated with a second case series comprising 89 individuals. The case series was compiled, masked to the modelling process, on the basis of sequential retrieval of the fields, derived with identical types of perimetry, from pre-designated diagnostic categories. There was no known selection bias**.** This second series comprised 23 individuals with FIAS and no previous exposure to vigabatrin; 49 with refractory FIAS exposed to vigabatrin of whom 19 had concomitant homonymous visual field loss; and 17 with a negative history of epilepsy, 5 of whom exhibited homonymous field loss, only; and 12 field loss due to primary open angle glaucoma. [35] Seventy-eight of the 89 pairs of fields met the inclusion criteria from which the reference VAVFL had been modelled [20] with the exception, where appropriate, of the inclusion of individuals with either homonymous or glaucomatous field loss. The remaining 11 pairs of fields were intentionally included on the basis of reduced quality in order to investigate the impact of symmetrisation on the evaluation of such fields. Two cases of advanced glaucomatous field loss were included to determine whether the algorithms could differentiate the loss from that arising due to severe VAVFL. The fields were evaluated in the same manner as for, but masked to, the locked data set.

RESULTS

Of the 89 individuals in the validation case series, 35 had undergone both the FF135 and the C30-2T, 18 the FF135 and 36 the C30-2T. The summary statistics of the demographics for each diagnostic category are given in Table 1.

Table 1 The demographics, type of perimetry, and frequency of visual field loss within the modelled and the validation case series

	Total	**Gender** Male: Female	**Age** Mean ± SD Median IQR Range	**VGB duration (Years)** Mean ± SD Median IQR Range	**VGB cumulative dose (Kg)** Mean ± SD Median IQR Range	**Type of perimetry** Number of individuals	**VAVFL / other type of loss** Number of individuals
Modelled VAVFL	123	50:73	40.8 ± 13.6 - - 17.0 - 75.0	9.1 ± 3.4 - - 0.2 - 16.1	8.13 ± 4.44 - - 1.4 - 19.5	FF135 + C30-2T; 63 FF135; 24 C30-2T; 36	58; - 17; - 20; -
FIAS no vigabatrin exposure	23	14:9	38.6 ± 11.0 38.0 28.5 - 44.5 18.0 - 59.0			FF135 + C30-2T; 23	-; -
High-functioning children with FIAS + vigabatrin exposure	8	4:4	12.6 ± 1.50 12.0 11.8 - 14.0 11.0 - 15.0	> 3/12		F135; 8	4; -
FIAS + vigabatrin exposure	22	10:12	44.4 ± 15.5 48.5 28.5 - 55.5 20.0 - 69.0	8.05 ± 4.18 8.00 5.08 - 10.98 0.92 - 16.05	6.65 ± 4.20 6.63 4.14 - 8.54 0.33 -16.73	FF135 + C30-2T; 2 FF135; 7 C30-2T; 13	2; - 5; - 8; -
FIAS + vigabatrin exposure + homonymous field loss	19	10:19	40.9 ± 11.5 39.0 36.0 - 51.0 21.0 - 58.0	7.38 ± 4.19 8.89 4.00 - 10.03 0.17 - 13.21	7.11 ± 5.67 6.30 2.16 - 8.51 0.19 - 18.12	FF135 + C30-2T; 10 FF135; 3 C30-2T; 6	9; 6Q, 4H 3; 2Q, 1H 1; 4Q, 2H
Homonymous field loss no epilepsy	5	2:3	- 35 - 19 - 42			C30-2T; 5	-; 5 Q
Primary open angle glaucoma	10	2:10	71.3 ± 7.6 73.0 67.0 - 77.3 58.0 - 80.0			C30-2T; 12	-; 12 G

Second row: (Modelled VAVFL): the case series from which the modelled reference fields were compiled. Subsequent rows: the validation case series. FIAS, focal impaired awareness seizures; H, homonymous hemianopia; Q, homonymous quadrantanopia; G, glaucomatous; VGB, vigabatrin; VAVFL, vigabatrin-associated visual field loss.

Outcome of the pattern recognition algorithms

The outcomes of the pattern recognition algorithms relative to the 'gold standard' clinical evaluation of the measured and symmetrised paired fields, derived with the FF135, for the individuals within each

diagnostic category of the validation case series, are shown in the left and the right columns, respectively, of figure 1 and for the C30-2T in figure 2. The outcomes of the algorithms across the entire validation case series are also tabulated in the online supplemental table S1.

The interpretation of the algorithms (figures 1 and 2) is undertaken in three stages. The first stage determines whether the distance of the measured (or the symmetrised, as appropriate) pairs of fields from the modelled reference pattern of VAVFL lies within ±3SD from the mean distance of the randomly generated pairs of fields (the light grey region between the dashed lines in figures 1 and 2). As noted previously, a value underneath 3SD indicates that the pairs of fields exhibit VAVFL beyond chance at $p<0.0015$. The second stage, as indicated by the magnitude of the ordinate, delineates the similarity of the measured pair of fields to that of the modelled reference pair of fields: as the value tends to zero the similarity increases. The third stage, as indicated by the magnitude of the abscissa, documents the severity of the field loss.

The algorithms exhibited excellent agreement with the clinical evaluations for both the measured and symmetrised paired fields. The sensitivity and specificity for the FF135 was 95.7% (95% CI 78.1% to 99.9%) and 100% (95% CI 88.4% to 100.0%), respectively. The positive predictive value (PPV) was 100% (95% CI 84.6% to 100.00%) and the negative predictive value (NPV) 96.8% (95% CI 81.5% to 99.5%). The algorithms correctly designated the presence of VAVFL in 22 of the 23 cases (4 of the 4 high-functioning children with refractory FIAS; 6 of the 7 adults with refractory FIAS; and all 12 with refractory FIAS and homonymous field loss). The ages of the 4 children with VAVFL were 11, 12, 14 and 14 years, respectively. The algorithms correctly designated the absence of VAVFL in all 30 cases (the 23 individuals with FIAS and no exposure to vigabatrin; the four high-functioning children with refractory FIAS and exposure to vigabatrin; the two individuals with refractory FIAS and exposure to vigabatrin; and the individual with refractory FIAS, exposure to vigabatrin, and homonymous field loss).

The sensitivity and specificity for the C30-2T was 94.4% (95% CI 72.7% to 99.9%) and 94.1% (95% CI 83.8% to 98.8%), respectively. The PPV was 85.0% (95% CI 65.3% to 94.5%) and the NPV 98.0% (95% CI 87.7% to 99.7%). The algorithms correctly designated the presence of VAVFL in 17 of the 18 cases

(all eight individuals with refractory FIAS; and 9 of the 10 individuals with refractory FIAS and homonymous field loss). They also correctly designated the absence of VAVFL in 48 of the 51 cases (all 23 individuals with FIAS; 5 of the six individuals with refractory FIAS and exposure to vigabatrin; all five individuals with refractory FIAS, exposure to vigabatrin and homonymous field loss; all five individuals with a negative history of epilepsy and homonymous field loss and 10 of the 12 individuals with glaucomatous field loss). Two individuals yielded fields of such poor quality as to render them clinically uninterpretable (Cases 36 and 57) and were not included in the analysis.

Symmetrisation was particularly useful in the presence of a disparity in the quality of the measured fields between the two eyes e.g., that arising from the perimetric learning (cases, 41, 42 and 45) or fatigue (cases 35, 39 and 43) effects which preferentially affect either the first or second measured field, respectively, or from a trial lens artefact in one of the measured fields (cases 34 and 44). Examples of the clinical benefit of symmetrisation are illustrated in Figures 3 and 4. Symmetrisation facilitated the visualisation of VAVFL in the presence of homonymous loss (Figure 3, right column). The symmetrised pair of fields are compiled from the VAVFL, if present, in the nasal field of the eye ipsilateral, and in the temporal field from the eye contralateral, to the homonymous loss.

As expected, symmetrisation did not remove a spatially similar artefact present in each of the pair of fields e.g. that arising from bilateral ptosis (cases 42 and 46).

The measured and symmetrised C30-2T fields of case 36 exhibited an apparent gross constriction resembling end-stage VAVFL but which had been confirmed, in clinic, to be functional.

The measured paired fields from each of the four children exhibiting VAVFL were identical, within the measurement error, to the corresponding measured paired adult fields (online supplementary material figure S2).

The algorithms for the C30-2T correctly designated 10 of the 12 cases of glaucomatous field loss as non-VAVFL. As expected, the two incorrectly designated cases (Cases 83 and 84) manifested advanced glaucomatous loss.

DISCUSSION

The output from the machine learning algorithms, described here, is readily apparent and immediately interpretable in that it is referenced to familiar concepts, that is, a population mean and 3SDs. The greater the distance from the mean of the population of randomly generated fields, the greater the confidence that the output represents 'true' VAVFL. A further strength of the technique is that the outputs from the algorithms required relatively small amounts of training data.

The simplicity and clarity of the rationale for the output from the algorithms, contrary to that from deep learning techniques, offers a structured approach to clinical interpretation and, thereby, patient management, which could benefit community (neuro)-ophthalmology. The algorithms can also provide valuable feedback to the clinician in the interpretation of VAVFL.

The approach described here is markedly different from deep learning techniques which have been widely applied to ophthalmology, such as neural networks, where the output is a challenge to interpret due to the intricacy of the neural network architecture and where extensive data sets are required to train the network[35]. The lack of understanding as to how the output is generated from such systems inhibits clinical acceptance and regulatory approval will require validation against traditional diagnostic outcomes.

Symmetrisation is a novel and useful augmentation for the visualisation of VAVFL. It delineated symmetrical loss between the two eyes and 'removed' the extraneous locations from both measured fields, but particularly those of the more anomalous field. A Symmetry Index [20] which quantifies the extent of the between-eye mirror image symmetry of the measured paired fields can be used as an adjunct tool for the identification of VAVFL. The outcome of the Symmetry Index for the individuals in the validation case series is illustrated in online supplemental figure S3. However, it must be stressed that symmetrisation is only an aid to interpretation of VAVFL. The first manifestation of VAVFL within the central field generally occurs inferior-nasally and the temporal region is only affected in the late stages. [19] With homonymous heminanopic loss and the sole use of the C30-2T, early manifestation of VAVFL will only be evident in the nasal field of the eye ipsilateral to the homonymous loss.

The eight children each yielded a reliable outcome to the FF135. Suprathreshold static perimetry is suitable for high-functioning children from approximately 10 years of age. Compared with standard automated perimetry, it is easier for the patient; exhibits less variability in response, particularly at the extremities of the field; and, generally, yields a more immediately discernible appearance of VAVFL. It is also less dependent upon the expertise of the perimetrist compared with standard automated perimetry or manual or semi-automated kinetic perimetry.

The apparent end-stage appearance of VAVFL, that is, a concentric defect extending to approximately 15º eccentricity from fixation, also resembles functional field loss. The reliability of such fields should always be challenged using feedback from the perimetrist concerning patient compliance; from observation of the mobility of the patient; and by confrontation testing of the fields. The algorithms will also never distinguish between advanced VAVFL, and that arising from end-stage open angle glaucoma or, for example, later-stage retinitis pigmentosa. However, with such conditions, evaluation of the fields is undertaken alongside the associated clinical findings and either a negative history of epilepsy or a positive history for vigabatrin.

The individuals comprising the case series from which the modelled fields were derived, and also those of the validation case series, were included on the basis of sequential retrieval of clinical notes.
The extensive vigabatrin exposures within the two case series (table 1) were beneficial in that they resulted in a proportionately large number of cases of VAVFL manifesting a wide range of severities.

Caution should be exercised in that the pattern recognition algorithms were developed solely for the consideration of VAVFL and not for the identification of field loss arising from other aetiologies. However, the concept could, with appropriate modifications, be applied to other types of symmetrical field loss; and to manual and semi-automated kinetic perimetry.

In conclusion, two novel machine-learning algorithms, with a readily apparent and immediately interpretable output, were constructed for the objective identification of VAVFL, determined with the EMA-approved perimetric protocol. They yielded excellent agreement with a ‘gold standard’ clinical consensus opinion. The agreement was further enhanced by symmetrisation of the measured paired

fields. Such algorithms could be used to augment the clinical decision-making process in the management of patients receiving vigabatrin and also to assist those unfamiliar with the characteristics of VAVFL.

Contributors

JMW and CK drafted the manuscript which was critically reviewed by PEMS. All authors contributed to the study design. The algorithms were developed by CK masked to the locked 'gold standard' clinical interpretation of the fields. JMW is solely responsible for overall content as guarantor of the fields.

Funding The authors have not declared a specific grant for this research from any funding agency in the public, commercial or not-for-profit sectors.

Patient consent for publication Not applicable

Ethics approval The study involves human participants. The Local Ethics Committee ruled that approval was not required for this study. The visual field assessments were considered to be part of normal good clinical practice and exempted this study. The study was conducted using data, previously obtained for clinical purposes, in accordance with the 1964 Helsinki Declaration and its later amendments or comparable ethical standards.

Provenance and peer review Not commissioned, externally peer reviewed

Data Availability The data are available on reasonable request.

to local regulations, clinical guidelines, terminology, drug names and drug dosages), and is not responsible for any error and/ or omissions arising from translation and adaptation or otherwise.

ORCID ID

John M Wild http://orcid.org/0000-0003-3019-3889

REFERENCES

1. Bresnahan R, Gianatsi M, Maguire M et al. Vigabatrin add-on therapy for drug-resistant focal epilepsy. *Cochrane Database Syst Rev* 2020;7:CD007302

2. Xu Z, Gong P, Jiao X, et al. Efficacy of vigabatrin in the treatment of infantile epileptic spasms syndrome: A systematic review and meta-analysis. *Epilepsia Open* 2023;8:268-77.

3. Maguire MJ, Hemming K, Wild JM, et al. Prevalence of visual field loss following exposure to vigabatrin therapy: a systematic review. *Epilepsia* 2010;51:2423-31.

4. Wild JM, Martinez C, Reinshagen G, et al. Characteristics of a unique visual field defect attributed to vigabatrin. *Epilepsia* 1994;40:1784-94.

5. Lawden MC, Eke T, Degg C, et al. Visual field defects associated with vigabatrin therapy. *J Neurol Neurosurg Psychiatry* 1999;67:716-22.

6. Wild JM, Robson CR, Jones AL, et al. Detecting vigabatrin toxicity by imaging of the retinal nerve fiber layer. *Invest Ophthalmol Vis Sci* 2006;47:917-24.

7. Lawthom C, Smith PE, Wild JM. Nasal retinal nerve fiber layer attenuation: a biomarker for vigabatrin toxicity. *Ophthalmology* 2009;11:565-71.

8. Clayton LM, Dévilé M, Punte T, et al. Retinal nerve fiber layer thickness in vigabatrin-exposed patients. *Ann Neurol* 2011;69:845-54.

9. Clayton LM, Devile M, Punte T, et al. Patterns of peripapillary retinal nerve fiber layer thinning in vigabatrin-exposed individuals. *Ophthalmology* 2012;119:2152-60.

10. Wild JM, Aljarudi S, Smith PEM, et al. The topographical relationship between visual field loss and peripapillary retinal nerve fibre layer thinning arising from long-term exposure to vigabatrin. *CNS Drugs* 2019;33:161-73.

11. Harding GF, Wild JM, Robertson KA, et al. Separating the retinal electrophysiologic effects of vigabatrin. Treatment versus field loss. *Neurology (E Cronicon)* 2000;55:347-52.

12. Westall CA, Wright T, Cortese F, et al. Vigabatrin retinal toxicity in children with infantile spasms: an observational cohort study. *Neurology (E Cronicon)* 2014;83:2262-68.

13. Buncic JR, Westall CA, Panton CM, et al Characteristic retinal atrophy with secondary "inverse" optic atrophy identifies vigabatrin toxicity in children. *Ophthalmology* 2014;111:1935-42.

14. Frisén L, Malmgren K. Characterization of vigabatrin-associated optic atrophy. *Acta Ophthalmol Scand* 2003;81:466-73.

15. Krauss GL, Johnson MA, Miller NR. Vigabatrin-associated retinal cone system dysfunction: electroretinogram and ophthalmologic findings. *Neurology (E Cronicon)* 1998;50:614-8.

16. Miller NR, Johnson MA, Paul SR et al. Visual dysfunction in patients receiving vigabatrin Clinical and electrophysiologic findings. *Neurology (E Cronicon)* 1999; 53:2082-7.

17. European Agency for the Evaluation of Medicinal Products. Opinion of the Committee for Proprietary Medicinal Products pursuant to Article 12 of Council Directive 75/319/EEC as amended for vigabatrin. Annex I Scientific conclusions and grounds for amendment of the summaries of product characteristics presented by the EMEA. https://www.ema.europa.eu/en/documents/referral/opinion-committee-proprietary-medicinal-products-pursuant-article-12-council-directive-75/319/eec-amended-vigabatrin-annexes-i-ii-iii-iv_en.pdf Accessed 23rd April 2024.

18. Malmgren K, Ben-Menachem E, Frisén L. Vigabatrin visual toxicity: evolution and dose dependence. *Epilepsia* 2001;42:609-15.

19. Wild JM, Fone DL, Aljarudi S, et al. Modelling the risk of visual field loss arising from long-term exposure to the anti-epileptic drug vigabatrin: a cross-sectional approach. *CNS Drugs* 2013;27:841-9.

20. Wild JM, Smith PEM, Knupp C. Objective derivation of the morphology and staging of visual field loss associated with long-term vigabatrin therapy. *CNS Drugs* 2019;33:817-29.

21. Hardus P, Verduin WM, Postma G, et al. Long-term changes in the visual fields of patients with temporal lobe epilepsy using vigabatrin. *Br J Ophthalmol* 2000;84:788-90.

22. Clayton LM, Stern WM, Newman WD et al. Evolution of visual field loss over ten years in individuals taking vigabatrin. *Epilepsy Res* 2013;105:262-71.

23. Johnson MA, Krauss GL, Miller NR, et al. Visual function loss from vigabatrin: effect of stopping the drug. *Neurology (E Cronicon)* 2000;55:40-5.

24. Nousiainen I, Mäntyjärvi M, Kälviäinen R. No reversion in vigabatrin-associated visual field defects. *Neurology (E Cronicon)* 2001;57:1916-7.

25. Heijl A, Lindgren A, Lindgren G. Test-retest variability in glaucomatous visual fields. *Am J Ophthalmol* 1989;108:130-5.

26. Wood JM, Wild JM, Hussey MK, et al. Serial examination of the normal visual field using Octopus automated projection perimetry. Evidence for a learning effect. *Acta Ophthalmol (Copenh)* 1987;65:326-33.

27. Hudson C, Wild JM, O'Neill EC. Fatigue effects during a single session of automated static threshold perimetry. *Invest Ophthalmol Vis Sci* 1994;35:268-80.

28. Heuer DK, Anderson DR, Feuer WJ, et al. The influence of refraction accuracy on automated perimetric threshold measurements. *Ophthalmology* 1987;94:1550-3.

29. Wall M, Woodward KR, Brito CF. The effect of attention on conventional automated perimetry and luminance size threshold perimetry. *Invest Ophthalmol Vis Sci* 2004; 45:342-50.

30. Kutzko KE, Brito CF, Wall M. Effect of instructions on conventional automated perimetry. *Invest Ophthalmol Vis Sci* 2001;41:2006-13.

31. Krauss G, Faught E, Foroozan R et al. Sabril® registry 5-year results: characteristics of adult patients treated with vigabatrin. *Epilepsy Behav* 2016;56:15-9.

32. Sergott RC, Johnson CA, Laxer KD et al. Retinal structure and function in vigabatrin-treated adult patients with refractory complex partial seizures. *Epilepsia* 2016;57:1634-42.

33. Foroozan R. Vigabatrin: lessons learned from the United States experience. *J Neuro-Ophthalmol* 2018;38:442-50.

34. Wild JM, Chiron C, Ahn H, et al. Visual field loss in patients with refractory partial epilepsy treated with vigabatrin: final results from an open-label, observational, multicentre study. *CNS Drugs* 2009;23:965-82.

35. Hodapp E, Parrish RK II, Anderson DR. Clinical decisions in glaucoma. St Louis: The CV Mosby Co; 1993.

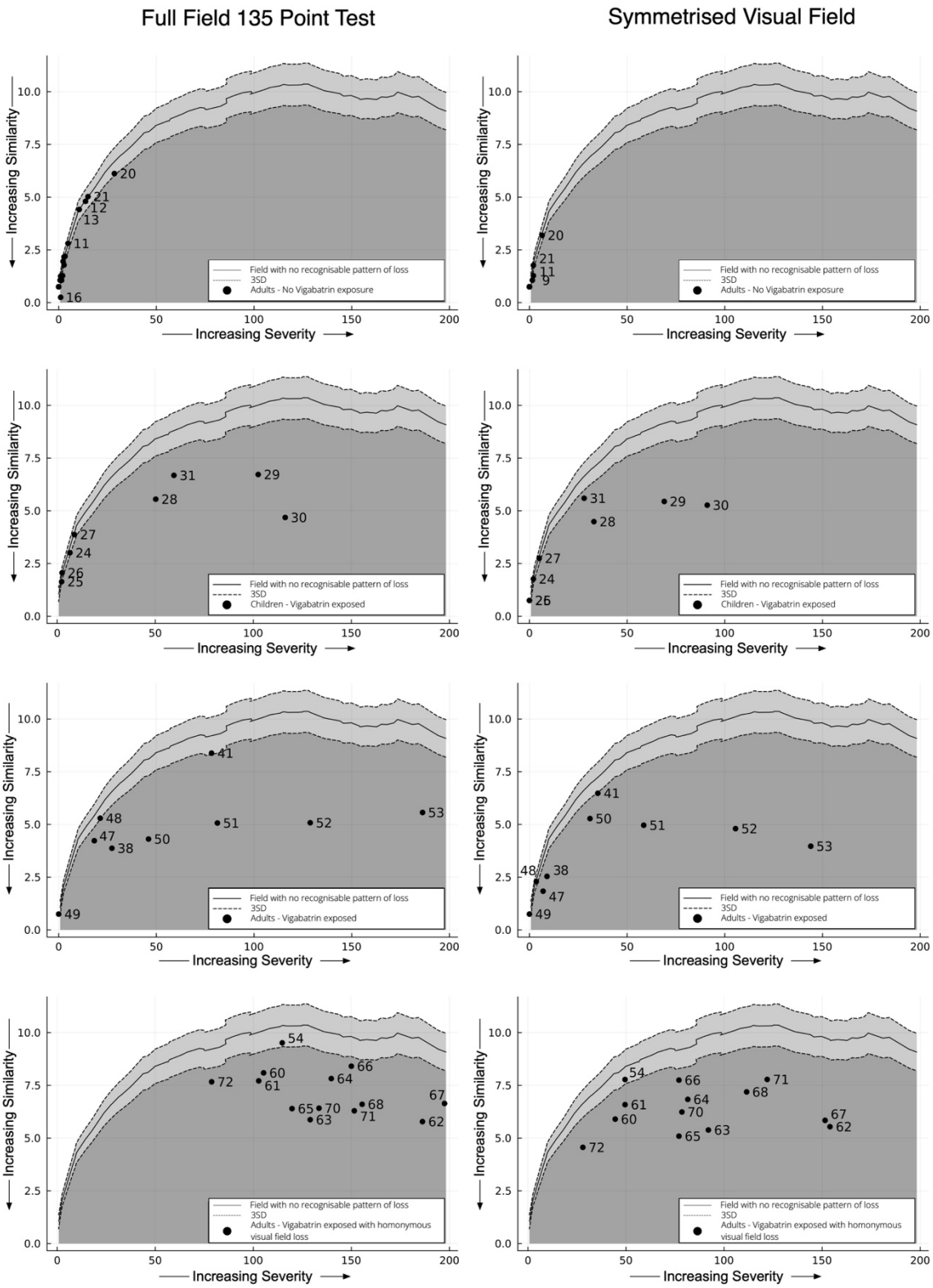

Figure 1 The pattern recognition algorithm for each transformed measured (left) and symmetrised (right) pair of fields obtained with the FF135. Each data point is accompanied by the corresponding Case Number of the individual. The light grey shaded region within the dashed lines (mean ± 3SDs) contains transformed pairs of fields which do not exhibit the characteristic reference pattern of VAVFL at any level of severity. Paired of fields below the lower dashed line, shaded dark grey, represents those with a probability of being a random event of <0.15% and, therefore, in this case, most likely to represent VAVFL. The abscissa represents the severity of the field loss (arbitrary units). The ordinate represents

the extent of the similarity between the measured/ symmetrised paired field to that of the characteristic reference pattern of VAVFL. For note, a point located above the upper dashed line represents a paired field which is distant from the reference field but which is not a random event, that is, the appearance is largely comprised of the opposite symbols to that of the reference field exhibiting VAVFL.

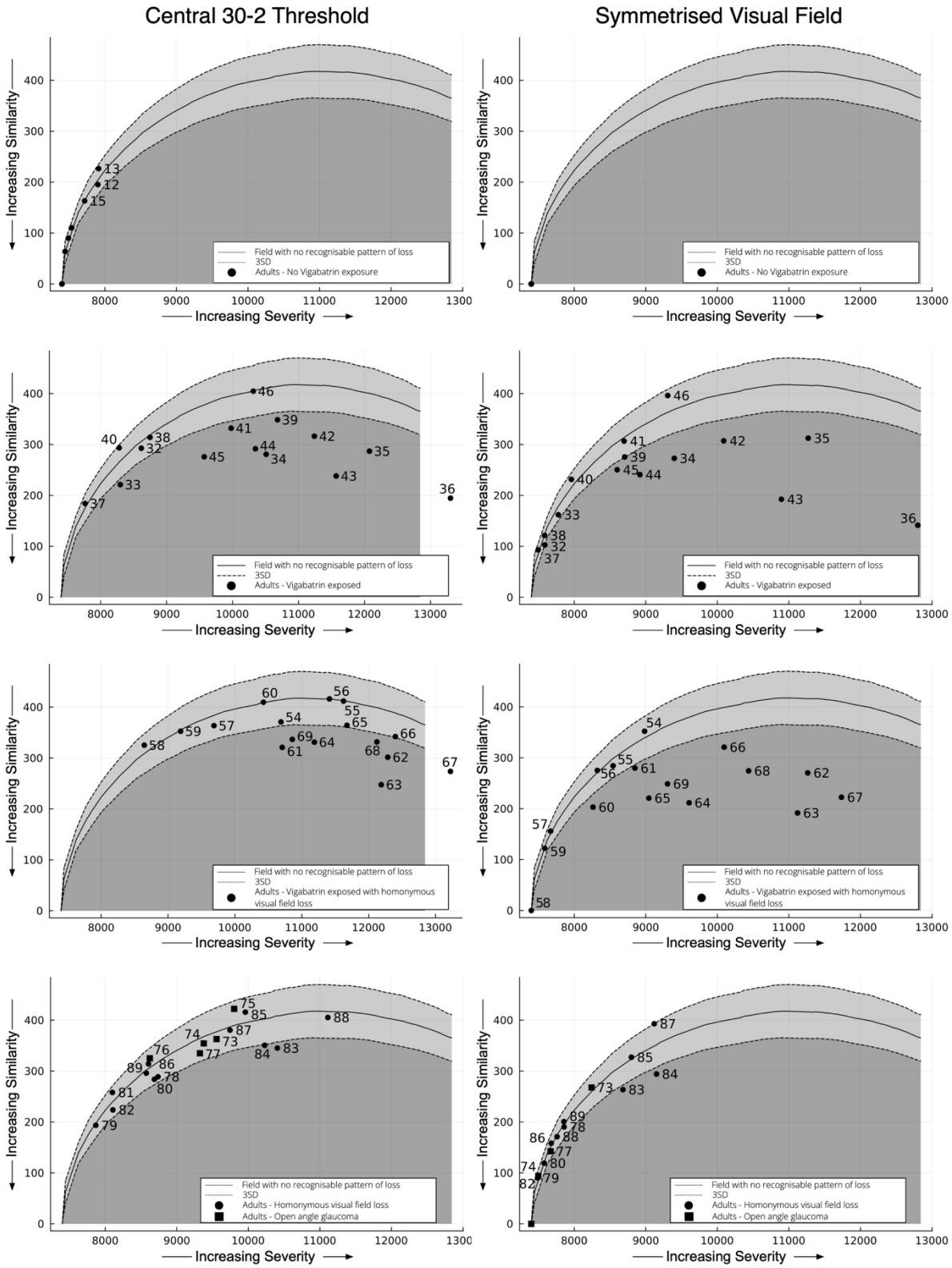

Figure 2 The pattern recognition algorithms for the transformed measured (left) and symmetrised (right) paired fields obtained with the C30-2T. The remainder of the figure caption/ legend is as described for Figure 1.

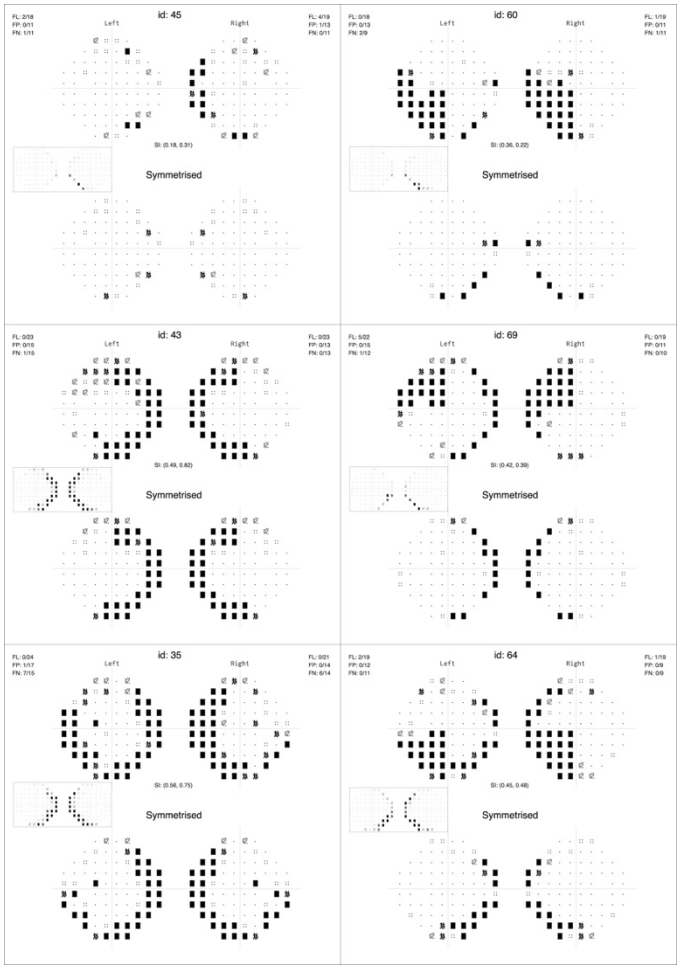

Figure 3 The clinical utility of the symmetrisation (bottom of each panel) for each of six cases exhibiting varying levels of severity of VAVFL in the measured paired field (top panel), as manifest in the Pattern Deviation Probability Map of the C30-2T, in the absence (left: cases 45, 43 and 35) and the presence (right: cases 69, 60 and 64) of homonymous visual field loss. The inset fields for each case represent similar measured paired fields from the case series of 123 individuals. VAVFL, vigabatrin-associated visual field loss.

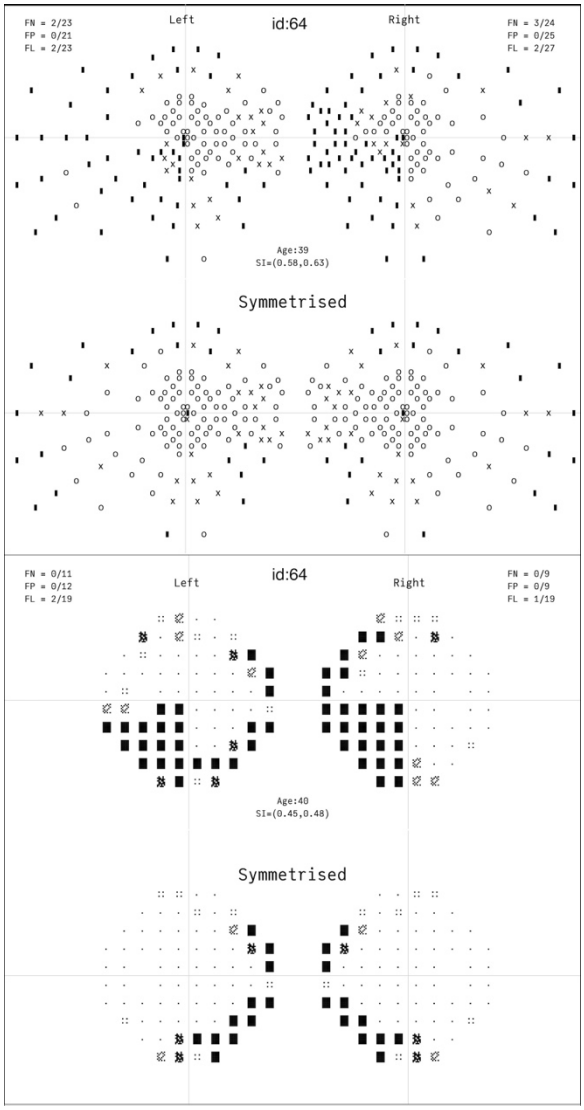

Figure 4 Comparison of the symmetrisation with the FF135 (top) and the C30-2T (bottom) for case 64 who manifested VAVFL in the presence of a left inferior quadrantanopia. The fields for the C30-2T are shown, previously, in figure ~~3~~ for comparison with others. VAVFL, vigabatrin-associated visual field loss.